

The process mineralogy of leaching sandstone-hosted uranium-vanadium ores

Molly R. Radwany^{1,2}, Isabel F. Barton^{1,*}

¹ Department of Mining & Geological Engineering, University of Arizona, Tucson, AZ

² now with Freeport-McMoRan Inc., Tucson, AZ

* corresponding author: fay1@arizona.edu

Abstract

In the United States, sandstone-hosted ore deposits of the Paradox Basin (Colorado Plateau) are major resources of uranium and vanadium, two metals important to green energy among other applications. Despite historic and current mining interest, and their significance as major domestic resources of critical elements, the geometallurgy of these deposits has received little study. This article documents the geometallurgy and process mineralogy of the U-V ores and identifies the principal barriers to optimal recovery by acid leaching.

Most of the metals occur as pitchblende (mixed uranium oxide-silicate), V hydroxides, V-bearing phyllosilicates, and diverse vanadates of U, Pb, Cu, and other metals. Commercial extraction is by two-stage heated tank leaching with H₂SO₄ and NaClO₃, yielding high U but lower V recovery (70-75% in the industrial operation). Laboratory leaching experiments coupled with comparisons of head and residue mineralogy indicate that the unrecovered U consists of micron-scale pitchblende grains locked within quartz and other insoluble minerals. The principal cause of suboptimal V recovery is the V-phyllosilicates, which show variable but generally poor solubility at room temperatures. An ancillary cause is locking of a small amount of fine-grained

24 V-hydroxide and pitchblende by authigenic quartz and V-phyllsilicates. Comparison with other
25 global V resources suggests that variable solubility of V-phyllsilicate ore minerals may also
26 diminish recovery from more common ore deposit types, such as V hosted in black shales or
27 stone coal, particularly in heap leaching of low-grade ores at coarse grain sizes.

28

29 **1. Introduction**

30 *1.1 Importance of uranium and vanadium*

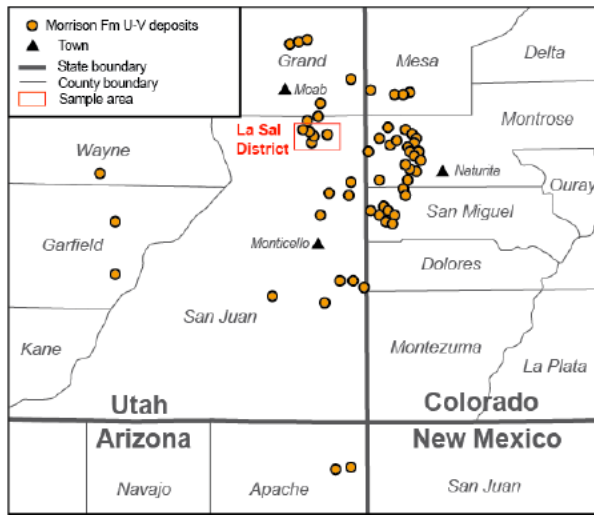
31 Uranium, an actinide, and vanadium, a first-row transition metal, are both major mineral
32 resources in the green energy transition. Both are considered strategic or critical elements in the
33 US: U for its nuclear potential and V as an ingredient in superalloy steels (Kelley et al., 2017;
34 Fortier et al., 2019). More recently, V has also garnered research interest for developing novel
35 batteries capable of storing the huge amounts of energy required for grid-scale implementation of
36 renewable energy.

37 Supply is a pressing problem for both metals. Recently the USA has imported most of its U
38 from Kazakhstan, Russia, and Canada, and most of its V from China and South Africa (US
39 Geological Survey, 2021). Rising demand for green energy and concerns over strategic metal
40 supply security are turning attention to available domestic resources. Some V can be produced
41 from spent oil-refining catalysts, power plant waste products, and steelmaking slags (US
42 Geological Survey, 2021). These yield no U and are not sufficient to meet the demand for V,
43 necessitating primary production.

44 The principal known resources of U and V in the USA are found in the Paradox Basin, a
45 roughly circular, uplifted basin on the Colorado Plateau (Fig. 1). Among the best-known and
46 largest historical producers were the mines in the Uravan Mineral Belt, which stretches across

47 eastern Utah and western Colorado. The only recent to current producers are mines in the La Sal
48 Creek district in Uravan, which produced 29 million pounds of V_2O_5 and an uncertain but large
49 amount of U_3O_8 between the early 1900s and 1980 (Kovschak and Nylund, 1981). Intermittent
50 production since 2006 has totaled > 8 M lbs V_2O_5 , and the district still contains 21.5 million lbs
51 of measured and indicated reserves and resources (Peters Geosciences, 2014).

52



53

54 Figure 1. Map of the Paradox Basin region, modified after Fischer (1942), showing the Salt
55 Wash-hosted U-V deposits and the La Sal district.

56

57 *1.2 Geological background*

58 The deposits in the La Sal district are mainly tabular orebodies occurring in quartz-
59 dominated sandstones of the Jurassic Salt Wash (lower Morrison) formation. Detailed geology of
60 the district is reviewed by Fischer (1942) and Carter and Gualtieri (1965), and the ores are
61 closely analogous to those of the Slick Rock district to the southeast, described in detail by
62 Shawe (2011). A more recent study by Barton et al. (2018) summarizes the petrography of other
63 Uravan deposits, as well as the historical research into their metallogenesis.

64 Ores in the Salt Wash belong mainly to the tabular subtype of sandstone hosted uranium-
65 vanadium deposits, although roll-front processes overprint and redistribute metals in some areas
66 (Burrows, 2010). Vanadium, and its common associate uranium, are most soluble in their
67 oxidized V(V) and U(VI) forms and precipitate mainly by reduction. The most likely reductant
68 in the Salt Wash deposits is H₂S, which occurs at high concentrations in Paradox Basin
69 petroleum plays and is one of the few geologically common species with enough reducing power
70 to precipitate montroseite ((V,Fe)OOH) (Wanty and Goldhaber, 1992). Montroseite is one of the
71 principal ore minerals, having precipitated along with pitchblende (a mix of uraninite [UO₂] and
72 coffinite [USiO₃ • nH₂O]) early in the sequence of ore deposition (Barton et al., 2018). During or
73 after the ore stage, some V was dissolved from montroseite and/or V in solution reacted with
74 authigenic quartz to form vanadian phyllosilicates such as roscoelite
75 (K(V,Al,Mg)₂AlSi₃O₁₀(OH)₂), V-illite (K_{0.65}(V,Al)₂(Al,Si)₄O₁₀(OH)₂), and V-smectite or V-
76 chlorite ((V,Fe,Mg,Al)₆(Si,Al)₄O₁₀(OH)₈), which occur as intergranular cements and fringes
77 around quartz grains. The last stage in the ore mineral paragenesis was supergene redistribution
78 of metals to form vanadates and other high-valent V(V) minerals (Barton et al., 2018). In detail,
79 the sequence of events and resulting mineralogy and mineral textures vary considerably within
80 deposits and individual orebodies. Table 1 gives the common minerals in the La Sal district U-V
81 ores. Accompanying gangue is mainly quartz (SiO₂), but includes potassic feldspar (KAlSi₃O₈),
82 calcite (CaCO₃), pyrite (FeS₂), and assorted minor metallic phases such as hematite (Fe₂O₃),
83 anatase (TiO₂), ferroselite (FeSe₂), clausthalite (PbSe), chalcopyrite (CuFeS₂), galena (PbS), and
84 jarosite (KAl₃(SO₄)₂(OH)₆).

85 Except for a few uranyl vanadates, virtually all of the U at La Sal occurs in pitchblende. In
86 terms of volume, the phyllosilicate minerals roscoelite, illite and chlorite are the most common

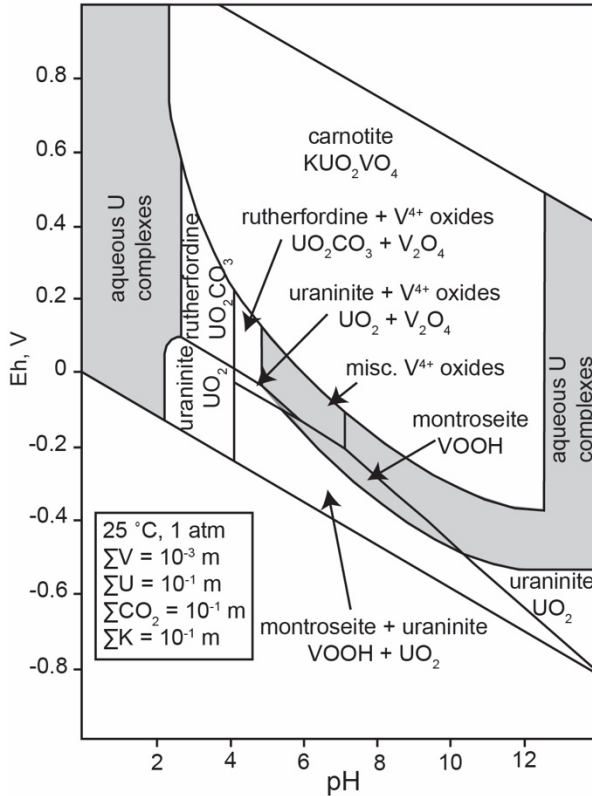
87 V-bearing phases, with the (hydr)oxides corvusite, montroseite, duttonite, and hewettite also
 88 occurring at multiple localities and hosting most of the recoverable V overall (Carter and
 89 Gualtieri, 1965). Most of these minerals deviate significantly from the ideal compositions in
 90 Table 1. The uraninite and coffinite that nominally comprise pitchblende in reality contain up to
 91 15 mol % U(VI) rather than pure U(IV) (Finch and Murakami, 1999). Similarly, Wanty et al.
 92 (1990) found that the oxidation state of both V and Fe in natural hydroxides such as montroseite
 93 is commonly mixed and highly variable with the average V(III)/V_{total} being 0.66 and the average
 94 Fe(III)/Fe_{total} being 0.62. Mixtures of V(III) and V(IV) in hydroxides may represent direct
 95 hydrolysis and precipitation of dissolved V(IV) in groundwater (Wanty et al., 1990), solid state
 96 oxidation and dehydration of montroseite to form paramontroseite (VO₂) (Evans, 1955; Forbes
 97 and Dubessy, 1988), and/or in-situ oxidation and hydration of montroseite to form duttonite
 98 ((V,Fe)O(OH)₂) (Thompson et al., 1957). A simplified Eh-pH diagram for U-V systems is shown
 99 in Figure 2.

100

101 Table 1. Principal ore mineralogy of the La Sal U-V deposits.

Oxides and Hydroxides	Silicates	Vanadates
Corvusite (Na,Ca,K) (V,Fe) ₈ O ₂₀ •4H ₂ O	Roscoelite K(V,Al,Mg) ₂ AlSi ₃ O ₁₀ (OH) ₂	Carnotite K ₂ (UO ₂) ₂ (V ₂ O ₈) •1-3H ₂ O
Duttonite (V,Fe)O(OH) ₂	V-chlorite (V,Fe,Mg,Al) ₆ (Si,Al) ₄ O ₁₀ (OH) ₈	Tangeite CaCu(VO ₄)(OH)
Hewettite CaV ₆ O ₁₆ •9H ₂ O	V-illite K _{0.65} (V,Al) ₂ (Al,Si) ₄ O ₁₀ (OH) ₂	Tyuyamunite Ca(UO ₂) ₂ (V ₂ O ₈) •5-8H ₂ O
Montroseite (V,Fe)OOH	Coffinite USiO ₃ • nH ₂ O	Uvanite U ₂ V ₆ O ₂₁ •15H ₂ O
Paramontroseite VO ₂		Vesigneite BaCu ₃ (VO ₄) ₂ (OH) ₂
Uraninite UO ₂		

102



103

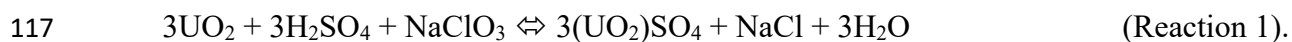
104 Figure 2. Simplified Eh-pH diagram for the K-U-V-C-O system, from Barton et al. (2018)
 105 and modified from Garrels et al. (1960).

106

107 *1.3 Metallurgical background*

108 Virtually anything oxidizing will dissolve U from uraninite and coffinite, and the presence of
 109 a carbonate, sulfate, organic, or other ligand stabilizes U in solution (Lunt et al., 2007; Bowell et
 110 al., 2011). Thus, hydrometallurgical methods have long been the preferred approach for U
 111 extraction. They have been recently reviewed by Schnell (2014) and Bhargava et al. (2015), and
 112 the electrochemical and kinetic details are provided by Nicol et al. (1975) among others. Briefly,
 113 leaching systems for U are always oxidizing, typically with NaClO₃, Fe³⁺ ion, or MnO₂ (Lunt et
 114 al., 2007). Acidic systems such as H₂SO₄ are the most common, but alkaline (NH₄)₂CO₃ is

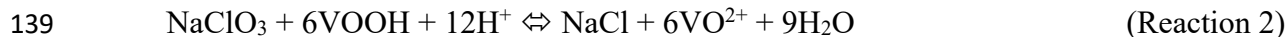
115 preferred for in-situ recovery or for leaching U in carbonate-rich deposits. A reaction for
116 uraninite leaching in sulfuric acid with sodium chlorate is:



118 Recoveries by acid leaching are high even when the ore is pitchblende rather than pure
119 uraninite. The major geometallurgical issues identified for U leaching in sandstone-hosted ores
120 are slower dissolution rates due to cationic impurities in uraninite (Ram et al., 2013); preg-
121 robbing by smectite, other clays, phosphates, and organic carbon (Lunt et al., 2007; Youlton and
122 Kinnaird, 2013; Pownceby and Johnson, 2014); and acid consumption by carbonates, which
123 raises pH and decreases dissolution rates (Eligwe et al., 1982; Youlton and Kinnaird, 2013).

124 By comparison, V is much more difficult to leach effectively and the reasons for its leaching
125 behavior are virtually unknown. Prior to the 1950s, most U-V ores were treated by salt roasting
126 rather than leaching in order to extract maximum V. In salt roasting, V ores are heated in an
127 oxidizing atmosphere to 750-840°C in the presence of NaCl (Burwell, 1961). This converts V
128 into soluble sodium vanadates (e.g., sodium orthovanadate, Na_3VO_4) and separates it from
129 accompanying metals (Burwell, 1961). The roasted ores are then leached in water or acid,
130 yielding typical recoveries of 83-90% (Burwell, 1961). By the late 1950s salt roasting of U-V
131 ores had fallen out of favor, since recovery of U was prioritized over V during the Cold War and
132 leaching was cheaper for that purpose (Gupta and Krishnamurthy, 1992). Today the majority of
133 sandstone-hosted U-V ores are crushed and directly leached in an agitated, heated $\text{H}_2\text{SO}_4 -$
134 NaClO_3 tank (Gupta and Krishnamurthy, 1992). The mixed pregnant leach solution is sent for U
135 solvent extraction first, and the raffinate from this step goes to V solvent extraction before being
136 recycled through the leaching system. An overall reaction for direct leaching of an idealized
137 montroseite under those conditions is:

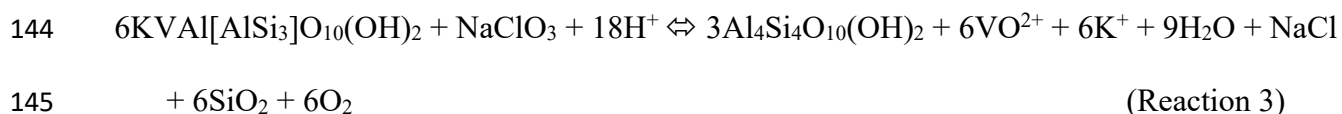
138



140

141 No reaction has yet been proposed for V leaching from phyllosilicates, but a plausible
142 reaction for an ideal roscoelite is:

143



146

147 This is hypothetical but would be consistent with the incongruent degeneration of micas
148 toward kaolinite compositions as observed in the oxidized acid leaching of copper (Baum, 1999).
149 A study by Tavakoli and Dreisinger (2014) examined the kinetics of synthetic vanadium oxide
150 (V_2O_5) leaching in sulfuric acid and found that VO_2 dissolves quickly but that its solubility is
151 relatively low. This leads to lower recovery at high solid-liquid ratios, exacerbated by decreases
152 in solubility with increasing pH and increasing temperature.

153 Geometallurgical issues in V leaching are not well understood, because most V is extracted
154 as a byproduct of steelmaking by non-hydrometallurgical methods. However, it is clear from
155 unpublished historical and present research that V leaching yields far lower recoveries than U
156 leaching in sediment-hosted ore types. Hazen Research performed metallurgical tests on low-
157 grade U- and V-bearing tailings from Naturita, Colorado (Hazen Research Inc., 1976). The head
158 grade of the test samples was 0.32% V_2O_5 , with the dominant ore minerals consisting of
159 tyuyamunite and roscoelite (Hazen Research Inc., 1976). Recoveries of V were < 40% from
160 agitated sulfuric acid leaching and sodium carbonate/carbonic acid leaching. The most successful

161 method was agglomeration of the tailings with sulfuric acid, followed by an overnight cure, and
162 then percolation of dilute sulfuric acid through the agglomerate at a rate of 0.01-0.02 gpm/ft²
163 (Hazen Research Inc., 1976). The reasons for the poor recoveries were not documented.
164 Recoveries at the White Mesa Mill, operating since 1980 on La Sal ores, are higher, at around
165 70-75%, but still considerably lower than the U recovery (96%) despite V grades generally being
166 much higher than U grades (Peters Geosciences, 2014). The mill has operated since 1980,
167 crushing and grinding ores to -600 µm followed by two-stage tank leaching in heated sulfuric
168 acid with a sodium chlorate oxidant (Baker and Sparling, 1981).

169 More recent published studies on V leaching are generally lacking due to the unique nature
170 of the deposits and the relative scarcity of active mining. The Colorado Plateau is one of very
171 few provinces worldwide in which sandstone U deposits contain significant V, so most research
172 on tabular U deposit geometallurgy omits discussion of V. Both U and V were produced in large
173 volumes from the Colorado Plateau during most of the 20th century, but mining in the region has
174 virtually shut down since the early 1980s. Research dwindled along with production, so studies
175 on the geometallurgy of V mainly shifted to slags, titanomagnetite deposits, stone coal, and other
176 feedstocks (e.g. Zheng et al., 2019a,b; Gilligan and Nikolski, 2020). Since such ores are
177 refractory to leaching, extraction is by salt roasting, which has thus become the main focus of
178 geometallurgical research on V in recent years (Peng, 2019). Thus, most references to the
179 geometallurgy of V in leaching date from the middle to late 20th century. A renewal of interest in
180 the Colorado Plateau U-V deposits, however, is underway, and may trigger additional
181 commercial and research activity (Mills and Jordan, 2021).

182

183 *1.4 Objective of this study*

184 This study aims to examine the geometallurgy of sandstone-hosted U-V ores in acid leaching
185 systems. A particular objective is to identify the causes of suboptimal V recovery during
186 leaching, through leaching experiments coupled with comparisons of head and tail mineralogy.
187 The implications are twofold. Firstly, this study will add an important new direction to the
188 literature on the process mineralogy of sandstone-hosted U ores. This has been a topic of
189 significant research, but almost all of it concerns V-poor deposits and the behavior of V minerals
190 in these leaching systems is thus almost completely unknown (Youlton and Kinnaird, 2013;
191 Youlton, 2014). Secondly, this study will shed light on geometallurgical problems in the
192 hydrometallurgy of V, a subject of increasing interest in settings including black shale or stone
193 coal. These low-grade but large V resources, like La Sal, host a considerable fraction of their V
194 as phyllosilicates. This study can therefore help elucidate the likely geometallurgical problems in
195 this type of unconventional V resource (Li et al., 2009, 2010).

196

197 **2. Materials and methods**

198 *2.1 Samples and sample preparation*

199 Six coherent rocks on the order of 1 cubic foot each were sampled from the Energy Fuels ore
200 stockpiles located on the Pandora Mine property. Each block was broken up by hammer and
201 individually bagged. The six samples were crushed and split at Freeport-McMoRan's Tucson
202 Technology Center. The material was stage-crushed to -850 μm and split using a rotary splitter.
203 For each sample, three 3-g splits of -850 μm material were mounted in epoxy and polished for
204 mineralogical analysis. A split of 120 grams of material from each sample was further ground to
205 -106 μm from which eight 10-gram splits were set aside for leach tests and others pulverized,

206 dissolved with 3-acid (nitric, hydrochloric, fluoboric) microwave digestion, and finally analyzed
207 with ICP-OES. Carbon was assayed by Leco furnace.

208

209 *2.2 Mineralogical analysis and identifications*

210 Thin sections taken for geological fieldwork were examined in transmitted- and reflected-
211 light petrography (Bos Orent, 2021). Head sample mineralogical mounts were analyzed using
212 reflected-light petrography and a Tescan TIMA3. The TIMA scans were performed at 25 kV
213 accelerating voltage, with a working distance of 15.0 mm and a pixel size of 5 μm . Leached
214 residues were mounted in epoxy, polished, and analyzed on a JEOL 6010LA benchtop scanning
215 electron microscope (SEM). Ore mineral compositions for both head and residue samples were
216 obtained using a Cameca SX100 electron probe microanalyzer (EPMA). For most EPMA
217 analyses a 2 μm beam was used to minimize alkali migration and hydrous mineral damage,
218 however a spot beam was used where grain size was especially small. Magnification of 10,000X
219 was used during analysis. The beam conditions were 15 kV voltage and 20 nA current. Standards
220 for each element were analyzed for calibration and peak fitting before and after each analytical
221 session. Standard compositions, detection limits, and other analytical conditions are given in the
222 Supplementary Material.

223 The two major V-hydroxide minerals, montroseite and duttonite, are difficult to distinguish
224 based on backscatter and chemical data despite being distinct in optical petrography. Table 2
225 compares their features. In this study, they were not distinguishable by TIMA or SEM and were
226 grouped together as V-hydroxides. On EPMA, the only discernable chemical difference between
227 montroseite and duttonite is the un-analyzable volatile (OH⁻) content, which shows up as lower
228 analytical totals, and the Na content (Thompson et al., 1957). The V/Fe ratio and Na content both

229 increase dramatically in analyses with analytical totals < 80%. This boundary is interpreted to
 230 indicate a structural (crystallographic) difference and is used as the cutoff to distinguish duttonite
 231 (analytical totals < 80%, > 0.9% Na, V/Fe > 10) from montroseite (analytical totals \geq 80%, low
 232 Na, V/Fe < 10) in this study. Oxygen percentages reported are calculated assuming all iron as
 233 Fe(II) and all vanadium as V(III) for purposes of consistency and comparison. In reality, V-
 234 hydroxides are known to contain Fe(II), Fe(III), V(III), and V(IV) with a variety of single and
 235 coupled substitution mechanisms (Evans and Mrose, 1955; Thompson et al., 1957; Forbes and
 236 Dubessy, 1988; Wanty et al., 1990).

237
 238 Table 2. Comparative features of montroseite and duttonite. (Analytical totals reported are for
 239 V₂O₃ and FeO, though most natural samples have mixed-valence V and Fe; see text for
 240 discussion.) Optical features are based on Weeks et al. (1953) and Thompson et al. (1957).

Physical Features	Montroseite VOOH		Duttonite VO(OH)₂	
Color (transmitted light)	<i>Opaque, black</i>		<i>Translucent, brown</i>	
Crystal Habit	<i>Acicular, blades, laths</i>		<i>Massive, platy or pseudomorphous</i>	
Cleavage	<i>Parallel to c-axis</i>		<i>Perpendicular to c-axis</i>	
Occurrence	<i>Embedded in quartz overgrowths or in radiating clusters</i>		<i>Pseudomorph of montroseite or massive and anhedral</i>	
Chemical Composition	Ideal VOOH	Observed (n=33)	Ideal VO(OH)₂	Observed (n=31)
Average V ₂ O ₃ *	89.3%	64.3%	74.2%	58.7%
Average FeO*	0	14.7%	0	11.7%
Average Al ₂ O ₃	0	2.1%	0	1.5%
Average Na ₂ O	0	0.1%	0	0.8%
Average K ₂ O	0	0.2%	0	0.7%
Average analytical total	89.3%	83.6%	74.2%	76.5%

241
 242 The distinctions among V-phyllsilicates are also somewhat ambiguous. This study uses the
 243 classification developed by Meunier (1994) based on the atomic proportion of octahedral V and
 244 the extent of K deficiency. A phyllsilicate with $V / (V + {}^{\text{vi}}\text{Al} + \text{M}^{2+}) > 0.5$ is defined as
 245 roscoelite, and one with $V / (V + {}^{\text{vi}}\text{Al} + \text{M}^{2+}) < 0.5$ is defined as V-muscovite. Either of these

246 compositions combined with an overall interlayer cation atomic charge of < 0.80 , i.e. K-deficient
247 species, are designated V-illite. The few sheet silicates with $(Mg + Fe) > Al$ are designated V-
248 chlorite.

249

250 *2.3 Experimental procedures*

251 The 10-g leaching splits of all six ore samples, ground to $-106 \mu\text{m}$, were subjected to a three-
252 hour agitated leach to evaluate the process mineralogy of leaching. A solution of 10 g/L H_2SO_4
253 and 1 g/L NaClO_3 in deionized water, representing the reagents used in industrial practice, was
254 placed in a 500 mL beaker with a magnetic stirring rod. Each leaching test used a solid-to-liquid
255 ratio of 5% solids to avoid saturating the solution in the beaker.

256 All chemicals used were reagent-grade from Sigma-Aldrich. One approximately 10-g split
257 for each ore sample was fully emptied into each beaker of solution. During the experiment the
258 beaker was covered with a watch glass to minimize splashing and evaporation. All tests were
259 performed at 25°C . Sample volumes of 3-5 mL were obtained after 10, 20, 30, 60, 120 and 180
260 minutes of active leaching time using a syringe equipped with a filter tip with a $1 \mu\text{m}$ pore size.
261 Filtered leach liquor samples were expelled into polypropylene test tubes and labeled with
262 sample number and leaching time. One drop of concentrated nitric acid was added to each vial of
263 leach liquor to stabilize elements in solution and prevent precipitation. After each 3-hour leach
264 session, the solid residue was filtered, rinsed in deionized (DI) water and air-dried for epoxy
265 mounting and mineralogical analysis.

266 For leachate analysis, each solution sample was diluted 250,000x using a 100 μL Eppendorf
267 pipette in a diluent of 2% HNO_3 . Samples LS04, LS05 and LS11 were diluted one week after the
268 leach experiments and samples LS01, LS02 and LS03 were diluted on the same day as the leach

269 experiments. Despite the acidic conditions, the formation of an orange precipitate (presumably
270 V_2O_5) was apparent in several samples from LS11, and these leach liquors (120 min, 180 min)
271 were not submitted for dilution and analysis. The rest of the diluted leach liquors were analyzed
272 for V, Ni, Zn, Pb, U, and Cu at the University of Arizona Economic Geology and Geometallurgy
273 lab on an Element2 ICP-MS. One nitric and seven sulfuric acid blanks, four multi-element
274 standards, and two U-V standards at concentrations from 0.2 to 10 ppb were made from certified
275 standard reference materials in the lab. Standards were run before and after the analyses of the
276 unknown samples; blanks were distributed at intervals through the analytical run and also
277 analyzed before the final standard run. Analytical results were corrected to final concentrations
278 using the standards and blanks.

279

280 **3. Results**

281 *3.1 Head sample compositions*

282 The six ore samples are quartz sandstones in which rounded quartz grains and minor
283 feldspar, lithic clasts, heavy detrital minerals, and coalified plant material are the detrital
284 constituents. Consistent with this lithology, whole-rock geochemical results from sandstone ores
285 of the same deposit contain from 57% to 81% SiO_2 (Bos-Orent, 2021). Quartz is the most
286 volumetrically abundant phase, comprising between 53 and 89% (Table 3). The V-phyllosilicates
287 comprise 9 to 31%, and V-hydroxides comprise from 1-18% of the sample volume. Uranium
288 minerals make up < 1% of the samples by volume, mainly as uranyl vanadates with
289 compositions corresponding to uvanite and carnotite-tyuyamunite mixtures. The only
290 pitchblende present consists of inclusions under quartz overgrowths. K-feldspar and calcite are
291 minor but consistently present in the samples (Table 3). In all cases, these results should be taken

292 to include substantial uncertainty due to the sampling statistics associated with automated
 293 mineralogy work.

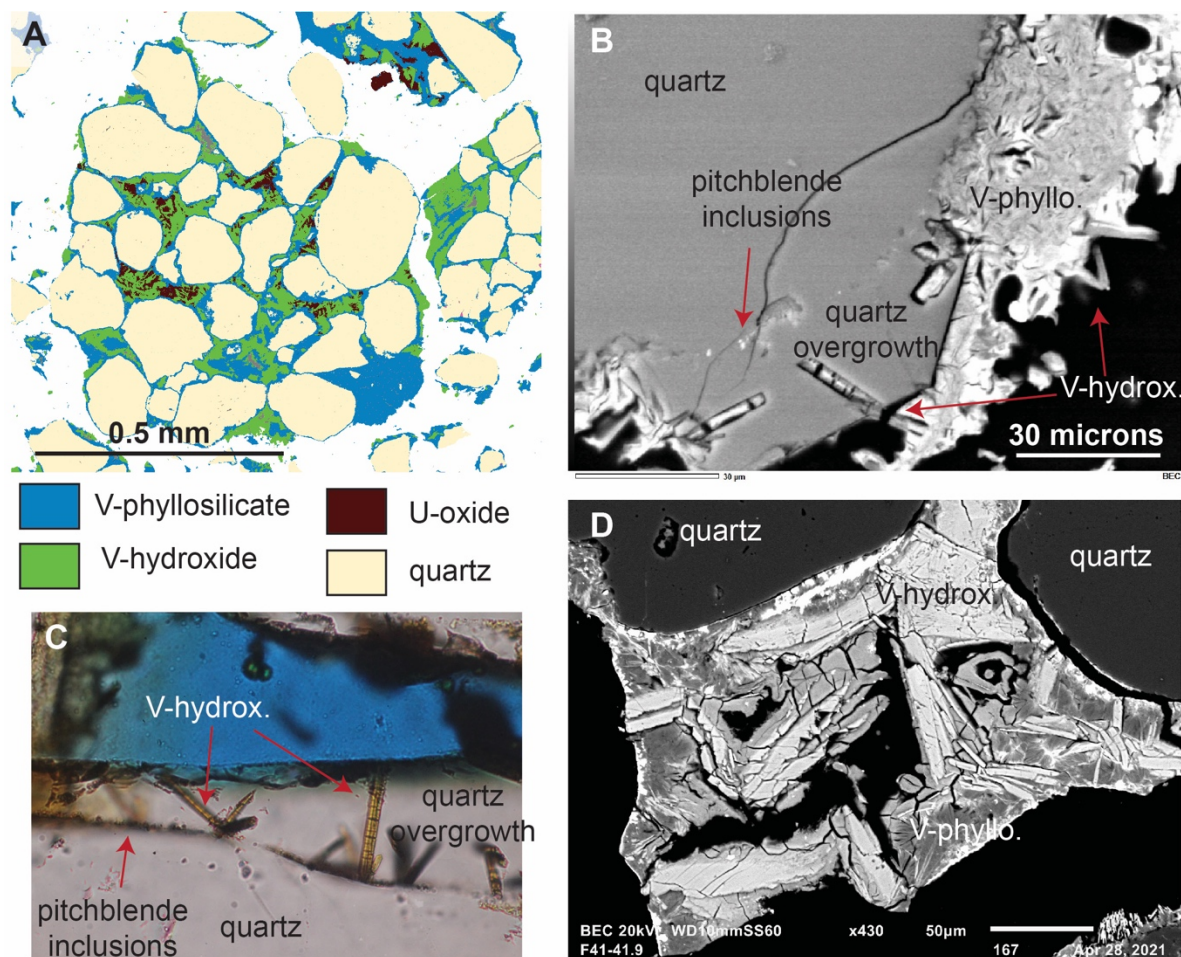
294
 295 Table 3. Modal mineralogy of samples in this study as determined by Tescan TIMA. Numbers
 296 show average and 1 standard deviation, based on three replicates analyzed for each sample. Dash
 297 indicates the phase occurs as less than 1% by volume. Phases detected at less than 1% in all
 298 samples are not listed. Vanadium deportments in the bottom row are approximate since V
 299 hydroxide and phyllosilicate compositions vary from sample to sample.

Phase	LS01	σ	LS02	σ	LS03	σ	LS04	σ	LS05	σ	LS11	σ
Quartz (%)	89.1	0.56	82.7	0.70	59.9	0.40	81.6	0.46	54.6	0.89	53.5	2.0
V-phyllosilicates (%)	8.9	0.50	12.6	0.42	27.9	0.60	14.8	0.37	23.0	0.41	30.9	1.5
V-hydroxide (%)	1.8	0.04	3.7	0.24	11.1	0.26	1.2	0.08	17.9	0.42	14.8	0.53
U minerals (%)	-	-	-	-	0.6	0.11	-	-	2.9	0.18	-	-
K-Feldspar (%)	-	-	-	-	-	-	1.1	0.09	-	-	-	-
All other phases (%)	0.19	0.01	1.02	0.07	0.48	0.01	1.23	0.04	1.58	0.29	0.84	0.02
% of total V in hydroxides	34.7		43.5		51.1		17.5		67.1		55.7	

300
 301 The diameter of quartz grains is 0.05 – 0.5 mm. Detrital grains are overgrown by euhedral
 302 quartz rims of 10-20 μm thickness. Partially or fully enclosed within the quartz rims are
 303 montroseite and pitchblende, some of which can also be found in the interstices between grains.
 304 Where the edges of quartz grains are ragged, suggesting dissolution, the grains are typically
 305 fringed by V-illite (proximal to quartz grain) and duttonite (distal to quartz grain) (Fig. 3). The
 306 V-illite also commonly contains anhedral quartz islands and necklace-like rings of tiny
 307 pitchblende grains that formerly marked the boundary between detrital quartz and quartz
 308 overgrowths. In addition to forming these rims around quartz grains, V-phyllosilicates also form

309 the main cement to the rock. Figure 3 shows representative photomicrographs of ore minerals
310 and textures.

311



312

313 Figure 3. Representative textures of the ores leached in this study (heads). A: TIMA image
314 showing a sample ground to -20 mesh. B: Backscattered SEM image showing occurrence
315 patterns of pitchblende as inclusions under quartz overgrowths; V-hydroxides enclosed within
316 quartz overgrowths and fringing V-phyllosilicates; and V-phyllosilicates as coronas around
317 corroded quartz overgrowths. C: Transmitted-light optical photomicrograph showing pitchblende
318 and V-hydroxides, in this case duttonite, locked in the overgrowth of a single quartz grain. D:
319 Backscattered SEM image showing V-hydroxides and phyllosilicates as interstitial species

320 between quartz grains. Variations in backscatter coefficient are caused by variable U, V, and Fe
 321 contents of the V-hydroxides and variable V contents of the phyllosilicates.

322
 323 Assay results for the six ore samples ranged from 1.87 – 10.37% V, 0.05 – 1.51% U and V/U
 324 ratio range from 6.9 to 37.6. Carbon and sulfur contents are below 2.5% and 1% respectively for
 325 each sample. Table 4 shows the percentages of the analyzed elements in the samples.

326
 327 Table 4. Select elemental assays of the six ore samples. b.d.l. = below detection limit. ACT =
 328 acid consumption.

Sample	LS01	LS02	LS03	LS04	LS05	LS11
Al (%)	0.65	1.17	2.39	1.97	2.07	2.62
C (%)	<i>b.d.l.</i>	0.06	0.03	<i>b.d.l.</i>	2.37	1.05
Ca (%)	0.06	0.47	0.18	0.09	0.17	0.16
Fe (%)	0.40	0.65	1.55	0.86	2.65	2.67
K (%)	0.31	0.56	1.06	0.34	0.97	1.30
Mg (%)	0.10	0.15	0.39	0.86	0.24	0.44
Na (%)	<i>b.d.l.</i>	<i>b.d.l.</i>	<i>b.d.l.</i>	0.08	<i>b.d.l.</i>	0.10
P (%)	0.01	0.02	0.03	0.01	0.03	0.02
S (%)	0.13	0.19	0.15	0.13	0.64	0.37
Ti (%)	0.02	0.06	0.07	0.15	0.04	0.07
U (%)	0.05	0.37	0.81	0.19	1.51	0.45
V (%)	1.95	2.98	7.23	1.87	10.4	10.1
Total ACT (lb/t)	114	158	251	87	306	285
V/U ratio	37.6	8.1	9.0	10.1	6.9	22.5

329
 330 *3.2 Vanadium mineral compositions*

331 Textural and compositional features apparent during petrographic, SEM and electron
 332 microprobe analysis indicated that the samples contained two different V-hydroxide minerals,
 333 identified as duttonite and montroseite in roughly equal proportions based on the cutoffs
 334 described above in Section 2.2. On average, duttonite contains about 40% V, and montroseite
 335 contains about 44% V, by weight (Table 2).

336 Three types of V-phyllsilicate were identified in this study using the criteria in Section 2.2:
337 roscoelite, V-illite, and V-chlorite. The V-illite and V-chlorite are fine-grained ($< 5 \mu\text{m}$) plates
338 and mostly occur within 5-20 μm -thick reaction rims around detrital quartz or as an intergranular
339 phase with quartz + V-hydroxide (Figure 4e). The atomic proportion of V in the La Sal V-illite
340 and V-chlorite samples from this study shows a negative linear correlation with Al, which is
341 taken to indicate that V(III) is primarily incorporated into the octahedral site of the silicate
342 structure (Foster, 1959; Meunier, 1994). In four of the six samples (LS01, LS03, LS05 and
343 LS11) the only V-phyllsilicate identified is V-illite. Sample LS02 contained a mix of roscoelite
344 and V-illite, and LS04 contained V-chlorite as the only phyllsilicate. Compositionally, the V-
345 illite analyzed in this study are very similar to those described by Meunier (1994) from other Salt
346 Wash localities. Representative compositions are given in Table 5.

347 A small amount of V also occurs in minor vanadate minerals making up $< 1\%$ of the rock by
348 volume. Uranyl vanadates occurred in most of the samples as a supergene alteration product.
349 Most are $< 10 \mu\text{m}$ in diameter and difficult to analyze, rendering identifications somewhat
350 tentative. Of those analyzed, the most common mineral appears to have the composition of
351 uvanite, followed by carnotite-tyuyamunite. Samples LS02 and LS04 also contain a few grains
352 of a Ti-Fe-V (hydr)oxide with V contents averaging 4%, but ranging as high as 20%. Based on
353 this composition, its occurrence, and common igneous exsolution textures, these grains appear to
354 be a detrital heavy mineral such as vanadiferous titanomagnetite. Only a few grains were
355 observed and their contribution to the overall V budget is negligible.

356

357 Table 5. Representative compositions of V-bearing minerals in La Sal head samples by electron
358 microprobe.

<i>Reduced & intermediate minerals (oxygen calculated assuming all V as V³⁺, Fe as Fe²⁺, and U as U⁴⁺)</i>								
Mineral sample	montr- oseite LS02	montr- oseite LS05	duttonite LS01	duttonite LS04	V-illite LS03	V-illite LS03	V-chlorite LS04	V-Ti-Fe oxide LS04
Analysis	2-17 20	5-4 1	12-2 15	2-17 57	12-7 17	5-4 54	2-17 49	2-17 41
Na	0.2	0.0	1.6	1.3	0.1	0.2	0.1	0.0
F	0.2	<i>n.a.</i>	0.1	0.0	0.1	<i>n.a.</i>	0.0	0.0
Mg	0.1	0.1	0.0	0.1	1.5	1.0	3.9	0.0
Al	0.9	1.1	0.5	0.3	8.3	7.4	8.6	0.1
Si	0.1	0.1	0.1	0.1	21.0	19.0	11.9	0.4
K	0.1	0.1	1.2	1.5	5.0	5.9	0.8	0.0
Ti	0.2	0.6	0.1	0.2	0.1	0.0	0.2	42.8
Ca	0.3	0.0	0.1	0.0	0.1	0.1	0.2	0.0
V ³⁺	43.0	45.3	37.7	39.2	9.8	16.0	16.0	4.0
Fe ²⁺	13.5	10.4	9.9	10.8	3.5	2.1	8.5	10.2
Mn	0.0	0.0	0.0	0.0	0.0	0.0	0.0	0.1
Cl	0.0	0.0	0.1	0.0	0.0	0.0	0.0	0.0
Ba	0.0	0.0	0.0	0.0	0.0	0.0	0.0	0.9
U ⁴⁺	0.1	0.0	2.5	0.0	1.2	0.6	1.9	0.0
O (calc)	25.4	25.8	22.4	22.9	39.3	38.4	34.4	34.1
Total	84.1	83.4	76.4	76.4	90.1	90.6	86.5	92.7
<i>Oxidized minerals (oxygen calculated assuming all V as V⁵⁺, Fe as Fe³⁺, and U as U⁶⁺)</i>								
Mineral, sample	Uvanite, LS01				Carnotite, LS03			
Analysis	12-7 34				12-7 21			
Na	0.4				0.1			
F	0.0				0.0			
Mg	0.1				0.0			
Al	1.0				0.1			
Si	0.1				0.1			
K	0.5				5.5			
Ti	0.0				0.0			
Ca	0.4				0.7			
V ⁵⁺	24.7				14.4			
Fe ³⁺	1.3				0.4			
Mn	0.0				0.0			
Cl	0.1				0.0			
Ba	0.0				0.0			
U ⁶⁺	34.6				48.1			
O (calc)	28.5				22.9			
Total	91.7				92.5			

359

360 *3.3 Leach test results*

361 Uranium removal was quantitative in samples with high enough U grades for reliable

362 measurement (LS05, see table 4) and no U minerals were observed in any of the residues except

363 for pitchblende under quartz overgrowths and minor U-enriched zones in clays. For V,
 364 recoveries are variable but all below 35% (Table 5). In the cases of LS05 and LS11, partially
 365 leached V-hydroxides were observed in the tails, suggesting that the low recoveries were due to
 366 the leach solution saturating in V. Recoveries in the industrial process are typically higher, most
 367 likely due to the use of multiple leaching stages (rather than single-stage beaker leaching) and
 368 the higher temperature.

369

370 Table 6. Results of leach tests from the samples in this study.

Sample	Assay %V	V recovery, %
LS01	1.95	34.2 ± 1.26
LS02	2.98	28.8 ± 0.94
LS03	7.23	27.7 ± 1.86
LS04	1.87	18.6 ± 0.76
LS05	10.4	33.2 ± 2.02
<i>LS11</i>	<i>10.1</i>	<i>25.6* ± 0.80</i>

371 *Precipitates were observed after sampling.

372

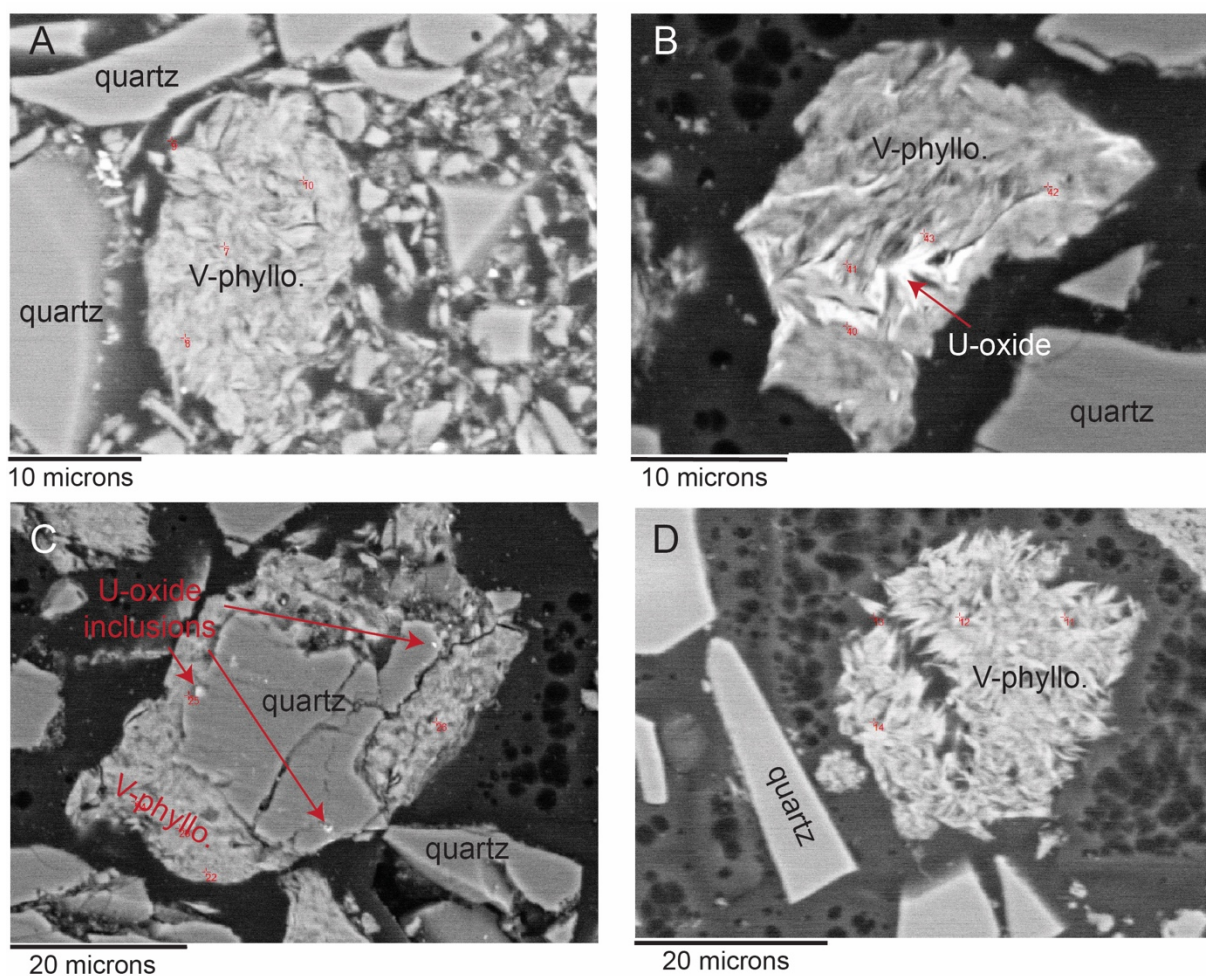
373 *3.4 Tails sample compositions*

374 Figure 4 shows the typical appearance of the leached tails. Analysis by SEM and EPMA
 375 shows that the leach residues consist primarily of angular quartz fragments up to 100 µm
 376 diameter and clumps of V-illite. Most of the V-illite clumps are ~10 µm in diameter with
 377 individual illite grains ~2 µm in length, however some clumps are as large as ~50 µm in
 378 diameter. This is somewhat larger than the typical occurrences in the heads and may reflect
 379 agglomeration during the leaching experiments. The only U phase observed in any of the tails
 380 was a minor U-enriched area in some of the clays, too fine to identify and volumetrically minor.
 381 Duttonite was identified in the tails from LS03 and LS05. The leached residues of other samples
 382 did not contain observed V-hydroxides. The duttonite in LS05 appeared to be partially leached,

383 with a ragged appearance and an average of 14% lower V than the duttonite in the corresponding
384 head. An exception was duttonite observed in the residue of LS03, which consisted of a single
385 clump of fine grains with no significant difference with the head in V content. Otherwise, the V-
386 hydroxides in LS03 were completely dissolved by leaching, so locking was probably the reason
387 for the residual duttonite.

388

389



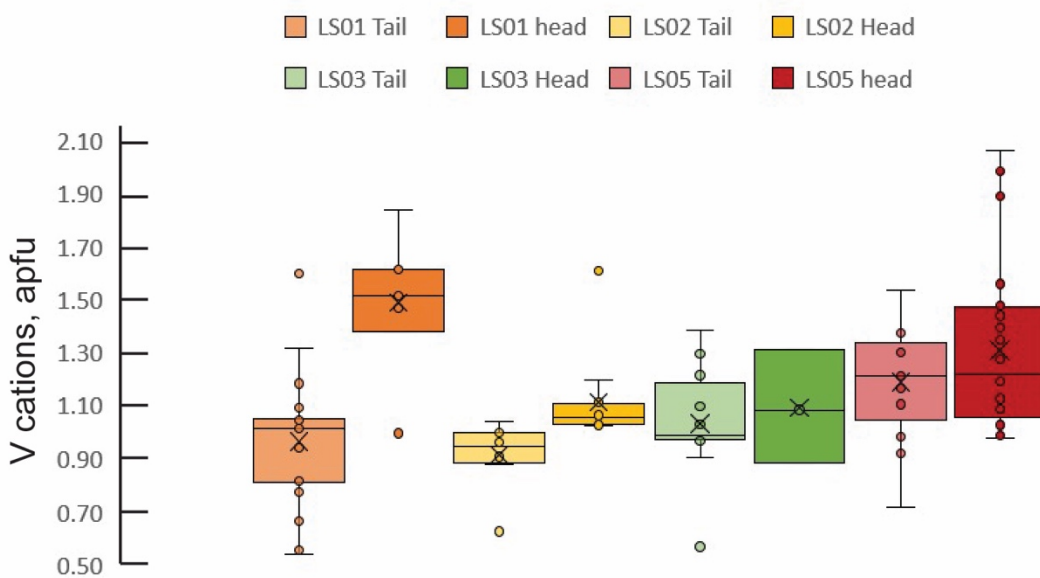
390

391 Figure 4. Representative textures of ore minerals found in the leached residues. A: Clumped V-
392 phyllosilicate loosely agglomerated with fine quartz grains. B: Fine U-oxide grains, probably

393 pitchblende, locked inside V-phyllsilicates and not leached. C: Preserved corona of V-
394 phyllsilicates around a quartz grain, also locking in U-oxide inclusions. D: Partially
395 disaggregated but unleached clump of V-phyllsilicates.

396
397 Comparison of V-illite compositions in corresponding head and tail (residue) samples
398 suggest that V leaching from V-illites is highly variable even within the same sample, with a
399 maximum of roughly 36% extraction in sample LS01 judging by the difference between heads
400 and tails (Fig. 5). Extraction of around 10% was achieved from the V-illites in LS02, and in no
401 other sample was there a statistically significant difference in the V content of the phyllsilicates
402 in heads and tails.

403



404
405 Figure 5. Box-and-whisker plot comparing V atoms per formula unit (apfu) V-phyllsilicate in
406 heads and tails.

407

408 **4. Discussion**

409 *4.1 Sources of decreased recovery*

410 This study identified two principal barriers to optimal recovery in the La Sal ores: locking of
411 highly soluble V-hydroxides and pitchblende in insoluble minerals, and the large proportion of V
412 hosted by low-solubility minerals, mainly V-illite and V-chlorite.

413 Locking is either by quartz overgrowths (pitchblende), or by clumps of V-illite (pitchblende,
414 V-hydroxides. It is apparent from SEM images of the -850 μm head mounts and the -106 μm tail
415 mounts that V-illite clumps are not fully disaggregated by grinding or by the agitated leach
416 process. High-resolution microscopy reveals that these clumps of V-phyllsilicate lock fine
417 grains of V-hydroxide and pitchblende (Fig. 4b,c). For U, physical locking appears to be the
418 principal cause of low recovery. However, for V it is less important than the low solubility of V
419 phyllosilicates.

420 Whereas the V-hydroxides leach readily when exposed, and are absent or nearly absent from
421 the tailings samples, V-phyllsilicates dominate much of the tails and retain most of their V. In
422 the SEM images of tail samples, V-illite is abundant and texturally intact, showing little evidence
423 of dissolution. Comparing EPMA analyses of V-illites in heads and tails showed reductions in V
424 content of only 3 – 36% (Fig. 5). The reasons for the variability in recovery from V-illite are a
425 subject for future investigation, but may relate to the varied siting and bonding structure of V in
426 phyllosilicates. The minor Ti-Fe-V oxide mineral also appears insoluble: grains of it were
427 identified in the tails containing up to 20% V, roughly the same concentration as in the heads.

428

429 *4.2 Effect of V-phyllsilicate type*

430 A mineralogical difference between the two lowest-grade samples – LS01 (1.95% V) and
431 LS04 (1.87% V) is likely to be one cause for their very different V recoveries. As discussed
432 above, in sample LS01 all available vanadium was leached from the V-hydroxide along with
433 approximately 1/3 of the vanadium contained in V-illite, yielding an overall recovery of 34.2%.
434 In contrast, sample LS04 yielded only 18.6% recovery despite identical leach conditions and
435 similar grade (Table 6). Vanadium in LS04 is hosted by V-chlorite (82.5% of V) and duttonite
436 (17.5% of V). The recovery of 18.6% is thus consistent, within error, with extracting more or
437 less all of the V from duttonite and none of it from the V-chlorite. Therefore, the type of V-
438 phyllosilicate in the deposit is likely to be important to leaching: V-chlorite appears to be very
439 resistant to leaching while V-illite yields higher, though still relatively low, recovery at the same
440 conditions.

441

442 *4.3 Comparison with previous studies*

443 Uranium ores in sandstone-hosted deposits and their metallurgy are both well-understood and
444 tractable (Youlton and Kinnaird, 2003; Pownceby and Johnson, 2014). The main process
445 mineralogy issues identified are acid consumption by carbonate gangue and preg-robbing by
446 phyllosilicates, organic carbon, and phosphates (Pownceby and Johnson, 2014; Youlton, 2014).
447 Neither of those was noted as a problem in this study. Pownceby and Johnson (2014) identified
448 locking by quartz as a problem for fine-grained pitchblende and suggested fine grinding to
449 liberate it, but the extremely small grain size of the pitchblende (Figs. 3 and 4) renders this
450 solution uneconomic for the La Sal ores.

451 By contrast, V in sandstone-hosted ores is rarer and is relatively poorly studied. The primary
452 example of the U-V deposit type outside the Paradox Basin is the Bigrlyi deposit in Australia,

453 whose ore and gangue mineralogy is virtually identical to La Sal's but whose metallurgy has not
454 been studied (Schmid et al., 2020). The literature that does exist on the metallurgy of sandstone-
455 hosted U ores, and of V in sediments, is mostly consistent with the results here for both U and V.
456 Recovery of U from pitchblende, and of V from hydroxides, is generally high (Peters
457 Geosciences, 2014; Tavakoli and Dreisinger, 2014). In contrast, recovery of V from
458 phyllosilicates is a well-known problem outside the Paradox Basin. The results presented here
459 are consistent with those of Li et al. (2009, 2010), who recovered < 80% of V from phyllosilicate
460 hosts in a black shale ore even with pressure leaching 130 °C and > 9 atm P_{O2}. At ambient
461 conditions, such as those in the present study, recoveries from V-phyllosilicates are generally far
462 lower, usually < 50%. Zheng et al. (2019a) suggested adding fluoride ion to the leaching solution
463 as a way to improve recovery from phyllosilicates, as the hydrofluoric acid (HF) that it forms is
464 one of the few acids capable of rapidly dissociating silicates. While their results did show
465 improved recovery in the leaching system, the overall viability of fluoride addition as a process
466 option is not clear given the environmental ramifications of HF formation.

467 The results of this study support previous investigations that have concluded that V recovery
468 from phyllosilicates varies with phyllosilicate type; however, the details are unresolved. Based
469 on density functional theory, Zheng et al. (2019b) suggested that V exists as V³⁺ in the
470 octahedral site of micas, and that the main control on leachability is whether the mica is
471 dioctahedral (muscovite) or trioctahedral (biotite). According to their calculations, V should be
472 easiest to leach in dioctahedral micas. However, the accompanying experimental data they show
473 do not clearly indicate the type of mica, and in at least one of the two analyses presented, the
474 given composition corresponds to a chlorite or clay rather than a mica (Zheng et al., 2019b). In
475 this study, the highest recoveries from the phyllosilicates were achieved from sample LS01,

476 which contained V as V-illite, and were lower in the V-chlorite-dominated sample. This
477 contrasts with Zheng et al.'s results, as V-illite is a K-deficient dioctahedral mica; V-chlorite is
478 not a mica but is more analogous to trioctahedral (biotite) than to dioctahedral (muscovite) types.
479 Chlorite has a T-O-T-O rather than a T-O-T structure, so its behavior may not be entirely
480 analogous to that of either mica anyway. The other V-illite-dominated samples yielded much
481 lower recovery, leaving open the possibility that the higher recovery from LS01 results from
482 unrecognized complicating factors below the resolution of the analytical techniques employed in
483 this study. At any rate, the significance of V-phyllosilicate type for V leachability is ambiguous
484 given the current state of research.

485

486 *4.4 Implications for leaching in industrial settings*

487 This study has identified the principal sources of sub-ideal leaching recovery from sandstone-
488 hosted U and V ores. Recommendations for addressing the problems are less simple. For
489 uranium, the main loss to tailings is caused by physical locking. Some losses are inevitable given
490 the extremely fine grain sizes of the lost grains in quartz (Fig. 4), which precludes the possibility
491 of increasing recovery through fine grinding. For pitchblende grains locked in phyllosilicate
492 clumps, increasing agitation speed or residence time in the tank leach may disaggregate the
493 locking grains enough to enhance recovery. However, improvements are likely to be minor given
494 the already high U recoveries and the small grain sizes of the locked ores.

495 For V recovery, the main hindrance is the insolubility of some of the ore minerals even when
496 fully liberated. This could potentially be addressed by chemical additives that are better than
497 H₂SO₄ at dissolving silicate minerals. Zheng et al. (2019a) has suggested fluoride for this
498 purpose. Unfortunately, fluoride and other silicate-dissolving additives are probably uneconomic

499 even apart from environmental considerations. A reagent capable of dissolving phyllosilicates
500 would probably also attack quartz and feldspar, which make up the large majority of the ore-
501 bearing rocks (Table 3). Without expensive pre-concentration of the ore minerals, a leaching
502 system using fluoride or other additives would encounter prohibitive gangue reagent
503 consumption. A more viable option may be to lengthen leaching times. The economics would
504 depend on the relative impact of decreased throughput compared to increased V recovery, but
505 costs would likely be far lower than those incurred by using a silicate-dissolving additive.

506

507 *4.5 Implications for U and V extraction in other deposit types*

508 The results of this study also carry implications for U and V geometallurgy beyond the
509 relatively narrow field of sandstone-hosted U-V ores. The extraction of V from phyllosilicate
510 ores is a concern for other types of ores, such as the low-grade but high-volume resources of
511 black shale found principally in China (Li et al., 2009, 2010; Kelley et al., 2017). Salt roasting is
512 most often recommended as the technique that yields maximum V recovery, but its expense
513 makes it uneconomic for much of the low-grade V resource. Leaching is probably the cheapest
514 way to process the ores (Zheng et al., 2019a,b). But the results given here, in conjunction with
515 the existing literature, suggest that V recovery from phyllosilicates is a considerably more
516 complex problem than is generally recognized. Further research will focus on disentangling the
517 influences of phyllosilicate type, V siting and bonding, crystallinity, and other factors on V
518 leaching.

519

520 **5. Conclusions**

521 Geometallurgical problems in sandstone-hosted U-V ores vary. For U, recoveries are
522 generally high, limited only by the locking of a very small proportion of fine pitchblende grains
523 under insoluble minerals, mainly quartz overgrowths and within clumps of V-phyllosilicates.
524 When exposed, pitchblende grains are highly soluble and leach easily; however, exposing the
525 extremely fine grains found in leach residues would require prohibitively fine grinding.

526 For V, the main problem is the insolubility of V-phyllosilicates. Grain size is typically larger
527 than for U and liberation is accordingly better, but V recoveries are lower than U recoveries. The
528 main reason for this is that a large fraction of the V resource is held in V-illite, roscoelite, and V-
529 chlorite. Leach recovery from V-illite and roscoelite ranges up to nearly 1/3, but is near zero
530 from the V-chlorites. The reason for the variation in V recovery from V-illite and roscoelite is
531 the subject of ongoing investigation, but may relate to variations in V siting and bonding. The
532 geometallurgy of V in these sandstone-hosted ores is expected to be similar to its behavior in
533 leaching other phyllosilicate- and (hydr)oxide-dominated ore types worldwide, including V in
534 stone coal or black shale deposits.

535

536 **Acknowledgments**

537 Thanks to Energy Fuels for providing samples, site and data access, and consultation for
538 this study, and to Freeport-McMoRan Inc. for chemical and XRD analyses and TIMA instrument
539 time. This research was made possible through the assistance of and helpful discussions with
540 many collaborators, especially Jinhong Zhang, Brent Hiskey, Maxwell Drexler, Ken Domanik,
541 Mary Kay Amistadi, Eytan Bos-Orent, Jason Kirk, Brandon Widener, Kyle French, Rodney
542 Saulters, Ortrud Schuh, Timo Groves, and Logan Shumway. Some field sample collection,

543 solution analyses, and microprobe time were supported by parts of NSF grants 17-25338 and 20-
544 45277.

545

546 **References**

547 Baker, C.E., and Sparling, D.K., 1981, Design and development of the White Mesa uranium mill,
548 Mining Engineering, v. 33, p. 382-385

549 Barton, M.D., Barton, I.F., and Thorson, J.P., 2018a, Paleofluid flow in the Paradox Basin:
550 Introduction, *in* Thorson, J.P., Paradox Basin fluids and Colorado Plateau copper, uranium
551 and vanadium deposits field trip, Society of Economic Geologists, Guidebook Series, v. 59,
552 p. 1-12

553 Barton, I.F., Barton, M.D., and Thorson, J.P., 2018b, Characteristics of Cu and U-V deposits in
554 the Paradox Basin (Colorado Plateau) and associated alteration, *in* Thorson, J.P., Paradox
555 Basin fluids and Colorado Plateau copper, uranium and vanadium deposits field trip, Society
556 of Economic Geologists, Guidebook Series, v. 59, p. 73-102

557 Baum, W., 1999, The use of a mineralogical data base for production forecasting and
558 troubleshooting in copper leach operations, Proceedings of the Copper 99 International
559 Conference: October 10-13, 1999, Phoenix, Arizona

560 Bhargava, S., Ram, R., Pownceby, M., Grocott, S., Ring, B., Tardio, J., and Jones, L., 2015, A
561 review of acid leaching of uraninite, Hydrometallurgy, v. 151, p. 10-24

562 Bos-Orent, E., 2021, Characterization of U(-V) deposits in the La Sal district, UT and CO and
563 their relationship to Paradox Basin fluid flow, Unpublished M.S. Thesis, University of
564 Arizona, Tucson, Arizona, retrieved from repository.arizona.edu

565 Bowell, R.J., Grogan, J., Hutton-Ashkenny, M., Brough, C., Penman, K., and Sapsford, D.J.,
566 2011, Geometallurgy of uranium deposits, Minerals Engineering, v. 24, p. 1305-1313

567 Burrows, D.R., 2010, Uranium exploration in the past 15 years and recent advances in uranium
568 metallogenic models: Society of Economic Geologists, Special Publication 15, v. 2, p. 599-
569 652

570 Burwell, B., 1961, Extractive metallurgy of vanadium, Journal of Metals, Vol. 13, p. 562-566

571 Carter, W.D., and Gualtieri, J.L., 1965, Geology and uranium-vanadium deposits of the La Sal
572 Quadrangle, San Juan County, Utah and Montrose County, Colorado, Geological Survey
573 Professional Paper 508, 81 p.

574 Eligwe, C.A., Torma, A.E., and Devries, F.W., 1982, Leaching of uranium ores with the H₂O₂-
575 Na₂SO₄-H₂SO₄ system, Hydrometallurgy, v. 9, p. 83-95

576 Evans, H.T., and Mrose, M.E., 1955, A crystal chemical study of montroseite and
577 paramontroseite, American Mineralogist, Vol. 40, p. 861-875

578 Evans, H.T., and Garrels, R.M., 1958, Thermodynamic equilibria of vanadium in aqueous
579 systems as applied to the interpretation of the Colorado Plateau ore deposits, Geochimica et
580 Cosmochimica Acta, v. 15, p. 134-149

581 Evans, H.T., 1959, The crystal chemistry and mineralogy of vanadium, in, Garrels, R.M. and
582 Larsen E.S., comps, Geochemistry and mineralogy of the Colorado Plateau uranium ores:
583 Geological Survey Professional Paper 320, p. 91-102

584 Finch, R., and Murakami, T., 1999, Systematics and paragenesis of uranium minerals, Reviews
585 in Mineralogy and Geochemistry 1999, p. 91-179

586 Fischer, R.P., 1942, Vanadium deposits of Colorado and Utah, Geological Survey Bulletin 936-
587 P, p. 363-394

588 Forbes, P., and Dubessy, J., 1988, Characterization of fresh and altered montroseite [V,Fe]OOH;
589 A discussion of alteration processes, *Physics and Chemistry of Minerals*, Vol. 15, p. 438-445
590 Fortier, S.M., Nassar, N.T., Lederer, G.W., Brainard, Jamie, Gambogi, Joseph and McCullough,
591 E.A., 2018, Draft critical mineral list – Summary of methodology and background
592 information, U.S. Geological Survey Open-File Report 2018-1021, 15 p.
593 Foster, M.D., 1959, Chemical study of the mineralized clays, in Garrels, R.M. and Larsen, E.S.,
594 Geochemistry and mineralogy of the Colorado Plateau uranium ores, U.S. Geological Survey
595 Professional Paper 302, p. 121-132
596 Garrels, R.M., 1960, *Mineral Equilibria at Low Temperatures*, Harper & Brothers, NY: 254 p.
597 Gilligan, R., and Nikoloski, A.N., 2020, The extraction of vanadium from titanomagnetites and
598 other sources, *Minerals Engineering*, Vol. 146, 106106
599 Gupta, C.K., and Krishnamurthy, N., 1992, Extractive metallurgy of vanadium, Amsterdam,
600 Elsevier.
601 Hazen Research Inc., 1976, Uranium and vanadium recovery from Naturita and Durango
602 Tailings: Interim progress report no. 1, Coltrinari, E.L., and Light, R.H., Preps, Unpublished
603 Report
604 Kelley, K.D., Scott, C.T., Polyak, D.E., and Kimball, B.E., 2017, Vanadium, chap. U of Schulz,
605 K.J., DeYoung, J.H., Jr., Seal, R.R., II, and Bradley D.C., eds., Critical mineral resources of
606 the United States – Economic and environmental geology and prospects for future supply:
607 U.S. Geological Survey Professional Paper 1802, p. U1-U36
608 Kovschak, A.A. and Nylund, R.L., 1981, General geology of uranium-vanadium deposits of Salt
609 Wash sandstones, La Sal area, San Juan County, Utah, *in* Epis, R.C., and Callender, J.F.,

610 New Mexico Geological Society, Thirty-second Field Conference, October 8-10, 1981, New
611 Mexico Geological Society Guidebook of the Field Conference Series, no. 32, p. 171-176

612 Li, M., Wei, C., Fan, G., Li, C., Deng, Z., and Li, X., 2009, Extraction of vanadium from black
613 shale using pressure acid leaching, *Hydrometallurgy*, Vol. 98, p. 308-313

614 Li, M., Wei, C., Qiu, S., Zhou, X., Li, C., and Deng, Z., 2010, Kinetics of vanadium dissolution
615 from black shale in pressure acid leaching, *Hydrometallurgy*, Vol. 104, p. 193-200

616 Lunt, D., Boshoff, P., Boylett, M., and El-Ansary, Z., 2007, Uranium extraction: the key process
617 drivers, *Journal of the Southern African Institute of Mining and Metallurgy*, v. 107, p. 419-
618 426

619 Meunier, J.D., 1994, The composition and origin of vanadium-rich clay minerals in Colorado-
620 Plateau Jurassic Sandstones, *Clays and Clay Minerals*, Vol. 42, No. 4, p. 391-401

621 Mills, S.E., and Jordan, B., 2021, Uranium and vanadium resources of Utah: an update in the era
622 of critical minerals and carbon neutrality, *Utah Geological Survey Open-File Report 735*, 26
623 p.

624 Nicol, M.J., Needes, C.R.S., and Finklestein, N.P., 1975, Electrochemical model for the leaching
625 of uranium dioxide, in Burkin, A.R., ed., *Leaching and Reduction in Hydrometallurgy*,
626 AusIMM, p. 1-11

627 Peng, H., 2019, A literature review on leaching and recovery of vanadium, *Journal of*
628 *Environmental Chemical Engineering*, Vol. 7, paper # 103313

629 Peters Geosciences, 2014, La Sal District Project NI43-101 Technical Report, 74 p.

630 Pownceby, M.I., and Johnson, C., 2014, Geometallurgy of Australian uranium deposits, *Ore*
631 *Geology Reviews*, v. 56, p. 25-44

632 Prophecy Development Corp., 2017, Gibellini Vanadium Project, Eureka County, Nevada, NI
633 43-101 Technical Report, Orbock, E.J.C., Prep.

634 Ram, R., Charalambous, F.A., McMaster, S., Pownceby, M.I., Tardio, J., and Bhargava, S.K.,
635 2013, An investigation on the dissolution of natural uraninite ores, *Minerals Engineering*, v.
636 50-51, p. 83-92

637 Schmid, S., Taylor, W.R., and Jordan, D.P., 2020, The Bigrlyi tabular sandstone-hosted uranium-
638 vanadium deposit, Ngalia basin, Central Australia, *Minerals*, v. 10, paper # 896

639 Schnell, H., 2014, Uranium processing practices, innovations, and trends, *in* Anderson, C.G.,
640 Dunne, R.C., and Uhrig, J., eds, *Mineral Processing and Extractive Metallurgy: 100 Years of*
641 *Innovation*, Society for Mining, Metallurgy, & Exploration, p. 457-465

642 Shannon, R.D., and Prewitt, C.T., 1969, Effective ionic radii in oxides and fluorides, *Acta*
643 *Crystallographia*, Vol. B25, p. 925-946

644 Shawe, D.R., 2011, Uranium-vanadium deposits of the Slick Rock district, Colorado, US
645 Geological Survey Professional Paper 576-F, 89 p.

646 Tavakoli, M.R., Dornian, S., and Dreisinger, D.B., 2014, The leaching of vanadium pentoxide
647 using sulfuric acid and sulfite as a reducing agent, *Hydrometallurgy*, Vol. 141, p. 59-66

648 Thompson, M.E., Roach, C.H., and Meyrowitz, R., 1957, Duttonite, a new quadrivalent
649 vanadium oxide from the Peanut Mine, Montrose County, Colorado, *The American*
650 *Mineralogist*, Vol. 42 p. 455-460

651 Thorson, 2018, Paradox basin fluids and Colorado Plateau copper, uranium and vanadium
652 deposits: overview, *in* Thorson, J.P., *Paradox Basin fluids and Colorado Plateau copper,*
653 *uranium and vanadium deposits field trip*, Society of Economic Geologists, *Guidebook*
654 *Series*, v. 59, p. 13-46

655 U.S. Geological Survey, 2021, Mineral commodity summaries 2021: U.S. Geological Survey,
656 200 p.

657 Wanty, R.B., Goldhaber, M.B., and Northrup, H.R., 1990, Geochemistry of vanadium in an
658 epigenetic, sandstone-hosted vanadium-uranium deposit, Henry Basin, Utah: Economic
659 Geology, v. 85, p. 270-284

660 Wanty, R.B., and Goldhaber, M.B., 1992, Thermodynamics and kinetics of reactions involving
661 vanadium in natural systems: Accumulation of vanadium in sedimentary rocks, *Geochimica
662 et Cosmochimica Acta*, v. 56, p. 1471-1483

663 Weeks, A.D., Cisney E.A. and Sherwood, A.N., 1953, Montroseite, a new vanadium oxide from
664 the Colorado Plateaus, *American Mineralogist*, Vol. 38, p. 1235-1241

665 Weeks, A.D. and Thompson, M.E., 1954, Identification and occurrence of uranium and
666 vanadium minerals from the Colorado Plateaus, *Geological Survey Bulletin 1009-B*, 62 p.

667 Weeks, A.D., Coleman, R.G., and Thompson, M.E., 1959, Summary of the ore mineralogy, in,
668 Garrels, R.M. and Larsen E.S., comps, *Geochemistry and mineralogy of the Colorado
669 Plateau uranium ores: Geological Survey Professional Paper 320*, p. 65-80.

670 Youlton, B., 2014, The process mineralogy of selected southern African uranium ores,
671 Unpublished Ph.D. thesis, University of the Witswatersrand, 370 p.

672 Youlton, B.J., and Kinnaird, J.A., 2003, Gangue-reagent interactions during acid leaching of
673 uranium, *Minerals Engineering*, Vol. 52, p. 62-73.

674 Zheng, Q., Zhang, Y., Liu, T., Huang, J., and Xue, N., 2019a, Vanadium extraction from black
675 shale: enhanced leaching due to fluoride addition, *Hydrometallurgy*, Vol. 187, p. 141-148.

676 Zheng, Q., Zhang, Y., Xue, N., Liu, T., and Huang, J., 2019b, Vanadium occupation and its
677 leachability differences in trioctahedral and dioctahedral mica, RSC Advances, Vol. 9, p.
678 27615-27624.
679